Development of closure models for unresolved particle simulations of heat and mass transfer in dense particle beds using CPPPO: a library for fast parallel data filtering

Federico Municchi[1], Christoph Goniva[2] and Stefan Radl[1] [*]

[1]*TU Graz, Institute of Process and Particle Engineering*
Inffeldgasse 13, 8010 Graz, Austria
fmunicchi@tugraz.at; radl@tugraz.at

[2]*DCS Computing GmbH*
Industriezeile 35, 4020 Linz, Austria
christoph-goniva@dcs-computing.com

Abstract

Most multiphase flows are characterized by a wide range of length scales at which processes of interest take place. Hence, closure models need to be used to account for small-scale phenomena, e.g., heat transfer from the particle surface to the surrounding fluid. We present a new open-source library for data filtering and processing named CPPPO (Compilation of fluid-Particle Post-PrOcessing routines) that aims on developing such closure models. This library has been designed as a universal tool for developing closure models in the context of single- and multiphase flows. CPPPO features a novel, highly efficient algorithm for on-the-fly parallel data filtering, and can be easily connected to any existing flow simulator with a minimum amount of coding. Furthermore, we make an attempt to derive a closure model for heat and mass transfer (from DNS data) to be used in unresolved CFD-DEM simulations.

Keywords: Gas-solid multiphase flows, direct numerical simulation, heat and mass transfer, poly-disperse particle beds, scale bridging, coarse grain models

1. Introduction

In this work we apply our novel library for parallel fluid-particle data processing (CPPPO) to explore the physics of heat and mass transfer in dense poly-disperse particle beds. In particular, we make use of particle-resolved direct numerical simulations (PR-DNS) to derive a closure model for particle-unresolved Euler-Lagrange simulations (PU-ELS). CPPPO is a tool developed to perform a *scale bridging* or *coarse-graining* (i.e., establishing correlations between phenomena occurring at different scales in the same system) by mean of closures for *coarse-grained models* [14]. With the term *coarse-grained models* we define those models used to solve a physical problem with a spatial resolution larger than the smallest scale of interest. For example, in PU-ELS the grid spacing is larger than the particle diameter and thus, all the information regarding the detailed fluid-particle interaction is lost. Consequently, closures have to be derived (e.g., from simulations that are able to predict all details of fluid-particle interaction) to account for a variety of phenomena, (e.g., fluid-particle momentum and heat transfer, pseudo-turbulent motion). This is generally accomplished by filtering the local fields with a suitable kernel function. PR-DNS has proven a valuable approach in this field allowing researchers to establish correlations for the dimensionless fluid-particle force [10] and the Nusselt (or Sherwood) number [4, 5, 16, 17, 18] in mono-disperse beds. Also, more recent studies evaluated the dimensionless fluid-particle force in poly-disperse beds [2, 8]. However, these studies mainly dealt with closures for continuum models (e.g., Two Fluid Models, TFM [1]), and hence are concerned with *average* fluid-particle interactions within an *ensemble of particles*. In contrast, in PU-ELS *individual* particles are described using a Lagrangian approach, and their motion is tracked using Newton's equation of motion, requiring particle-particle and fluid-particle interaction models on an *individual particle level*.

The main difference, from the point of view of the coarse-graining process, is that the filter size is generally much smaller when dealing with closure models for PU-ELS. In addition, the flow field experienced by each particle in a PU-ELS (of a moderately dilute to dense fluid-particle system) is always strongly inhomogeneous. This is in contrast to the assumption of classical TFMs, in which the particles are assumed to be homogeneously distributed within a single computational cell. We note that recently-developed *filtered* TFMs account for inhomogeneities on a sub-grid level [15, 11]. Most important, it is now widely accepted that closures for these filtered TFMs must depend on the filter size. In the same spirit we anticipate that closure models for *individual particles*, i.e., that for PU-ELS, must depend on the size of the filtered region. Our current contribution attempts to give an answer if this is indeed the case.

2. The CPPPO library

CPPPO is a library that features novel algorithms for filtering data from single- and multiphase flow simulations. Most important, CPPPO allows easy filter operation customization, making it easy for users to extract data for different filter sizes. In addition, CPPPO can perform other kinds of statistical operations like *sampling* and *binning* of filtered and unfiltered data, as well as of their derivatives (see Figure 1). CPPPO is linked to a fluid flow simulator, e.g., OpenFOAM®, by means of an interface class. More information about CPPPO, as well as a link to the source code, can be found at our Institute's web page.

In the present work we use CPPPO to evaluate filtered quantities (of the fluid flow field) at the particle position in order to com-

pute statistics of *local* fluid-particle interactions (e.g., particle-based Nusselt numbers). In particular, we are interested in Favre-averaged quantities of the fluid flow field, i.e.,

$$\widetilde{\psi^f}\left(\mathbf{x},t\right) = \frac{\int K\left(\mathbf{x}-\mathbf{x}',t-t'\right)\phi^f\left(\mathbf{x}',t'\right)\psi\left(\mathbf{x}',t'\right)d\mathbf{x}'dt'}{\int K\left(\mathbf{x}-\mathbf{x}',t-t'\right)\phi^f\left(\mathbf{x}',t'\right)d\mathbf{x}'dt'} \tag{1}$$

Where ψ is a scalar field (or a component of a vector field), K is the Kernel function and ϕ is the phase fraction. The superscript f indicates that the quantity is related to the fluid phase, and the integral is evaluated over the support of the kernel function. In the current study, we use a top-hat time independent kernel which is defined as:

$$K\left(\mathbf{x}-\mathbf{x}',t-t'\right) = \delta\left(t-t'\right)\prod_i\frac{\mathcal{H}\left(\frac{\Delta_i}{2}-|x_i-x_i'|\right)}{\Delta_i} \tag{2}$$

Being Δ_i the filter length in the i-th direction, δ the Kronecker delta function and $\mathcal{H}$ the Heaviside function. This kernel is particularly useful since it mimics the effect of a volume averaging process inherent to finite volume methods.
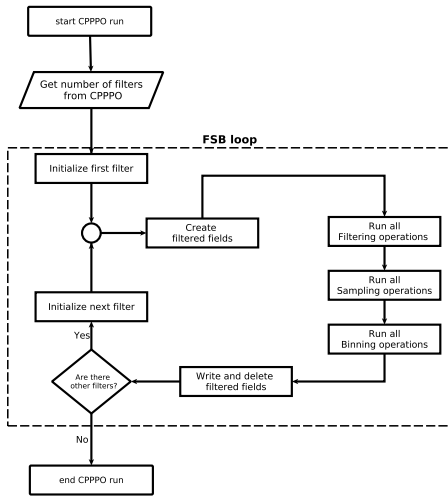

Figure 1: A typical CPPPO run consists of sequentially performing filtering, sampling and binning operations (i.e., the FSB loop) for every filter size.

3. Study description and numerical method

In this work we use CFDEMCoupling[R] [9] that combines the particle simulator LIGGGHTS[R] with the fluid flow simulator OpenFOAM[R], to perform PR-DNS.

3.1. Governing equations

In this work we solve the dimensionless incompressible Navier-Stokes equations together with a transport equation for a non-reactive scalar (e.g., the normalized temperature). Particle boundary conditions are imposed via a direct forcing immersed boundary method:

$$\frac{\partial u_i}{\partial x_i} = 0 \tag{3a}$$

$$\frac{\partial u_i}{\partial t} + \frac{\partial\left(u_j u_i\right)}{\partial x_j} = -\frac{\partial p}{\partial x_i} + \frac{1}{Re}\frac{\partial^2 u_i}{\partial x_j \partial x_j} + f_{IB} \tag{3b}$$

$$\frac{\partial\theta}{\partial t} + \frac{\partial\left(u_i\theta\right)}{\partial x_i} = \frac{1}{Pe}\frac{\partial^2\theta}{\partial x_i \partial x_i} + Q_{IB} \tag{3c}$$

Where u_i is the i-th component of the dimensionless flow field, p is the dimensionless pressure field (with $U^2\rho_f$ being the reference pressure), θ is the dimensionless temperature field, Re is the Reynolds number and Pe is the Peclet number. f_{IB} and Q_{IB} are the momentum and heat forcing term imposed by the immersed boundary method, respectively.

The definition of Re and Pe requires the definition of a reference length in poly-disperse particle beds, which is obviously the particle diameter in a mono-disperse bed. Thus, $Re = Ud_p/\nu$ for a mono-disperse bed, where U is a reference velocity, d_p is the particle diameter and ν is the kinematic viscosity of the fluid. In fact, the definition of an equivalent particle diameter for a poly-disperse particle *bed* has been debated in literature. However, a rigorous definition of a "poly-disperse" Reynolds number is only useful in case we are interested in closure models for TFMs. In PU-ELS, however, every particle experiences a local Re_p that is defined by its diameter and the Favre averaged (particle-relative) velocity field at its position. Similarly, we define $Pe = RePr$, where Pr is the Prandtl number. In our study we set $Pr = 1$ and thus $Re = Pe$. Furthermore, we limit our study to $Re = 10$. A quantity of particular interest in poly-disperse beds is the Sauter mean diameter. In case we define a volume-weighted inverse diameter:

$$\chi_i = \frac{\phi_i^p}{\phi_{tot}^p d_i} \tag{4}$$

Where ϕ_i^p is the volume fraction of particles with diameter d_i and $\phi_{tot}^p = \sum_i \phi_i^p = 1 - \phi^f$. The Sauter mean diameter can be written as:

$$\bar{d}_s = \left(\sum_i \chi_i\right)^{-1} \tag{5}$$

Where the sum is over all particle classes i.

The simulation is carried out in a fully periodic domain where the flow field is imposed by a pressure gradient. While this box setting works fine for studying a statistically homogeneous field (like the velocity field in a particle bed), a statistically non-homogeneous field, like the temperature field, will saturate in the flow direction.
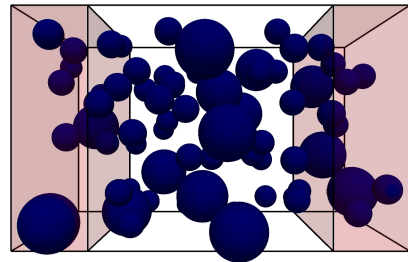

Figure 2: A bi-disperse bed with $\phi^f = 0.9$. A mean flow field is imposed from left to right, and a heat sink is applied at the left periodic boundary. Regions where filtering operations could lead to crossing the periodic streamwise boundary are coloured in red. Particles located in these regions are excluded from our analysis.

In addition, filtering operations cannot be carried out across the periodic boundary in the flow direction. Therefore, the domain is shaped in such a way to allow a certain maximum filter

size without crossing the flow-wise periodic boundary (see figure 2). Also, a heat sink is applied to impose a fixed bulk temperature at the periodic inlet. Finally, we need to make an assumption on the particles' velocity distribution. Specifically, in the present work we disregard the relative motion between particles, and hence set the particle velocity to zero.

3.2. Immersed boundary approach and forcing

In this work, we make use of a newly implemented HFD-IB (Hybrid Fictitious-Domain Immersed-boundary) algorithm to impose Dirichlet boundary conditions at particle surfaces. The algorithm reconstructs the temperature field near the surface of every particle using a second-order polynomial. This reconstruction is used to identify a target value which is then imposed using a Lagrangian multiplier fictitious domain approach. The method has been verified for several cases like the forced convection around a steady sphere (for results see figure 3). We also compared the results obtained with the HFD-IB solver against a body fitted mesh simulations as shown in figure 4.
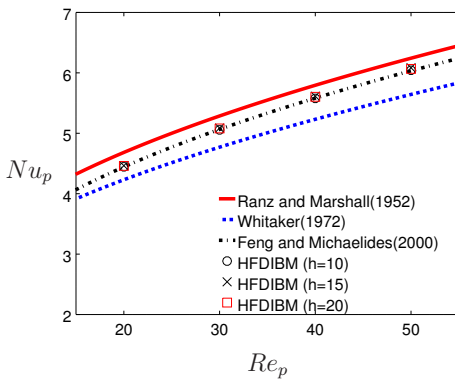

Figure 3: Comparison of results from the HFD-IB method and available literature data on forced convection around a sphere. Our solver agrees very well with the computational work of Feng and Michaelides [6], and deviates slightly from other literature data [19, 13]. In the figure h denotes the number of grid cells per particle diameter.

3.3. Numerical details

The governing equations are solved using second order discretization methods in space and time. Pressure coupling, and the immersed boundary forcing update are performed using a semi-implicit PISO-IB method [3]. A grid sensitivity analysis showed that a resolution of 20 cells per particle diameter is sufficient to represent the flow field around a particle. Thus, in each simulation, we adapted our grid resolution to resolve the smallest particles. Also, we made use of a fully structured hexahedral Cartesian grid with no grid refinement. The OpenFOAM® interface provided in the CPPPO package is already provided with the necessary functions to read data from CFDEMCoupling®, also in parallel. Details with respect to the domain decomposition (e.g., data transfer across processor boundaries) are detailed in [12].

4. Results

In the present contribution we limit our study to $Re = 10$, and we consider bi-disperse particle beds with a voidage of $\phi^f = 0.9$ and $\phi^f = 0.5$. Furthermore, for each case we consider situations with $\chi_1/\bar{d}_s = 0.5$, and $\chi_1/\bar{d}_s = 0.7$. The former case represents a situation where particles with diameter d_1 have the same surface-to-volume ratio as the particles with diameter d_2.
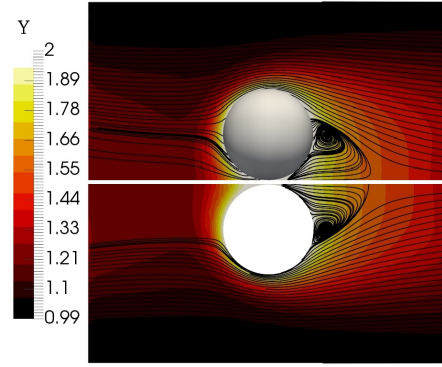

Figure 4: Dimensionless temperature field and streamlines for the case of forced convection around two particles. The upper panel shows one half of the results obtained with the HFD-IB solver, while the lower panel shows results from a simulation using a body fitted mesh. The HFD-IB solver overpredicts the particle-fluid heat transfer rate by approximately 3% compared to the body fitted simulation.

The latter case (i.e., $\chi_1/\bar{d}_s = 0.7$) favors the particles with d_1 from the point of view of the available exchange surface area. Next, we need to decide which marker to use for correlating fluid-particle interactions (e.g., the Nusselt number). CPPPO allows to obtain several statistics from the DNS data, and hence offers a variety of markers for this purpose. We choose the particle-based Reynolds number defined as:

$$Re_p = \frac{\widetilde{|u|}_p \overline{\phi^f}_p d_p}{\nu} \tag{6}$$

Where the $\overline{\phi^f}_p$ is the volume-averaged voidage in a filter region centered at the particle's position. We find that the distribution of Re_p has a mean value close to Re defined above, and a standard deviation that decreases with increasing filter size. Furthermore, the particle-based Nusselt number is evaluated from:

$$Nu_p = \frac{q_p^* Pr Re_p}{\theta_s - \widetilde{\theta}_p} \tag{7}$$

Where q^* is the dimensionless particle-fluid heat flux. θ_s is the dimensionless particle surface temperature and $\widetilde{\theta}_p$ is the Favre-averaged dimensionless fluid temperature in a filter region centered at the particle's position. Clearly, in a PU-ELS both Re_p and $\widetilde{\theta}_p$ are available, and q_p^* needs to be predicted based on a correlation for Nu_p. We next aim on establishing such a correlation for the small particles (i.e., that having the diameter diameter d_1) in the bi-disperse suspension. Regarding the particles with larger diameter, we cannot draw any conclusion at the moment, due to the comparably small number of samples for Nu_p. Clearly, simulations with a much larger number of particles are required to obtain enough statistics for particles with the diameter d_2.

First, we observe that for the dilute cases ($\phi^f = 0.9$) no saturation phenomena occur, i.e., the filtered temperature is always significantly lower than the particle surface temperature.

Second, we see that for dense beds the flow saturates quickly (see figure 5). Unfortunately, data from saturated regions cannot be used in the analysis. This is because the heat flux and the particle-fluid temperature difference is very small, and hence the computed Nusselt number is connected to significant noise. This leads to severe difficulties in establishing a particle based Nusselt number in case of a large particle concentration and low Peclet numbers. This is especially true for the small particles, since the filter size (i.e., the size of the corresponding coarse cell) should

Table 1: Ensemble averaged Nu_p for different dimensionless filter sizes $\rho = \Delta_i / d_1$ (small particles)

	$\rho = 2$	$\rho = 3$	$\rho = 4$	$\rho = 5$
$\chi_1 d_{s,p} = 0.7$	4.97	4.95	4.82	4.72
$\chi_1 d_{s,p} = 0.5$	5.11	6.48	6.25	6.02

be small. Hence, filtering is restricted to regions close to the domain inlet, which means that the bed should have a rather short extension into the main flow direction in case of large particle concentrations.
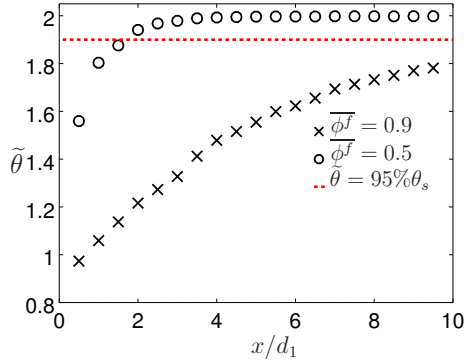

Figure 5: Favre-averaged dimensionless temperature over the bed length. The averaging is performed over the whole bed in the span-wise direction. The red dashed line represents the limit of saturation ($\widetilde{\theta} = 95\%\theta_s$). In both cases, the value of $\widetilde{\theta}$ at the periodic inlet is imposed equal to 1.

Third, we observe from our results that the dependence of Nu_p vs. Re_p is different from what we get in mono-disperse beds. Specifically, Nu_p experiences lower values, and a steeper gradient with respect to the particle-based Reynolds number as shown in figure 6. We notice that the larger the filter size, the more our data aggregates around $Re_p = Re$. This is caused by two factors, the first one being the fact that we choose d_1 to be our reference length (this explains why numerically converges to Re). A second factor is that u and ϕ_f are statistically homogeneous and thus, their Favre averaged values become more similar with increasing filter size.

Finally, we observe that the mean value of the particle-based Nusselt number is generally decreasing with increasing filter size (see table 1). The equivalent value from Gunn [7] (considering $\overline{\phi^f}_p = 0.9$ and $Re_p = 10$) is $Nu_{Gunn} = 5.04$. In principle, one could speculates that there is a correlation between the Nusselt number for bi-disperse beds and the one for mono-disperse beds. This correlation should have a form similar to (we omit the dependence on Pr for simplicity):

$$Nu_p \left(Re_p, \bar{\phi^f}_p\right) \approx Nu_{Gunn}\left(Re_p, \bar{\phi^f}_p\right) \Gamma\left(Re_p, \chi_p d_{s,p}\right) \quad (8)$$

Where $d_{s,p}$ is the mean Sauter diameter resulting from filtering around particle p and $\Gamma\left(Re_p, \chi_p d_{s,p}\right)$ is a correction function. Even though we do not know the functional for of Γ, equation 8 should return the mono-disperse Nusselt number in case there are just particles with the same diameter inside the filtered region, i.e., $\Gamma = 1$. Such a correlation would account for the contribution of different particle species with respect to their relative exchange surface. However, the definition of the particle-based Reynolds number to be used in the mono-disperse Nusselt number correlation (e.g., that of Gunn) is not obvious since it should represent the overall heat transfer rate inside the filtered region

from a single particle. A possible solution would be to define an equivalent mono-disperse Nusselt number based on the Sauter mean diameter as in [8]:

$$Re_p = \frac{\widetilde{|u|}_p \overline{\phi^f}_p d_{s,p}}{\nu} \quad (9)$$

Unfortunately, our current data set (limited to $Re = 10$) does not allow us to suggest which of the above mentioned approaches is more suitable for predicting local particle-based Nusselt numbers in a poly-disperse particle bed. However, our simulation results clearly suggest that poly-dispersity leads to significantly smaller heat transfer rates (from small particles) as one would estimate based on existing correlations for mono-disperse beds.
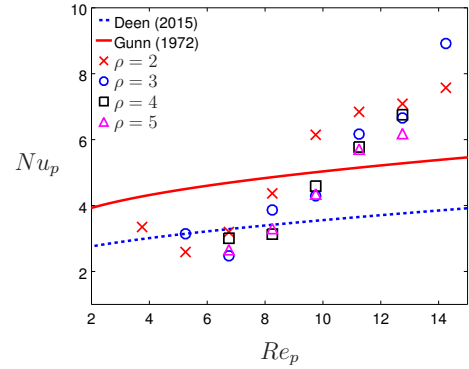

Figure 6: Computed Nu_p as a function of Re_p for the case where $\chi_1 / \bar{d}_s = 0.7$. In this configuration, the value of $\overline{\phi^f}_p$ is fluctuating around $\overline{\phi^f}_p = 0.9$ with a deviation that decreases with increasing filter size. We compare results from different filter sizes with existing correlations for mono-disperse beds from Gunn [7] and Deen [5] (we used $\overline{\phi^f}_p = 0.9$ for these correlations).

Finally, another interesting observation is that when sampling the small particles (i.e., that with diameter d_1), we observe that the ratio $\chi/\bar{d}_s$ is constant with the filter size. This is likely to occur due to the homogeneous particle distribution in the bed and may be related to the independence of our results on the filter size.

5. Conclusions

In this work we showed how the CPPPO library can be applied to the problem of heat transfer in bi-disperse particle beds. The outcome of this study is limited due to the low number of cases considered and by the effects of temperature saturation in dense beds. However, we show that the average Nusselt number (of small particles) has a value closer to the one predicted by Gunn [7] rather than Deen [5] and increase with decreasing $\chi_d/\bar{d}_s$. Thus, one should consider correcting existing correlations in case of a poly-disperse particle bed in order to improve predictions of the Nusselt number. Interestingly, we observed that the particle-based Nusselt number tends to decrease slightly

with increasing filter size (less than 7% from $\rho = 3$ to $\rho = 5$). Whether this is a consequence of the (statistically) homogeneous particle distribution in our simulations or not needs to be probed in future studies.

References

[1] Anderson, T. B. and Jackson, R. O. Y. A Fluid Mechanical description of fluidized beds. *Industrial and Engineering Chemistry Fundamentals*, 6(4):527–539, 1965.

[2] Beetstra, R. Drag Force of Intermediate Reynolds Number Flow Past Mono- and Bidisperse Arrays of Spheres. *IFAC Proceedings Volumes (IFAC-PapersOnline)*, 7(2):405–410, 2009.

[3] Blais, B., Lassaigne, M., Goniva, C., Fradette, L., and Bertrand, F. A semi-implicit immersed boundary method and its application to viscous mixing. *Computers and Chemical Engineering*, 85:136–146, 2016.

[4] Deen, N. G., Kriebitzsch, S. H. L., van der Hoef, M. a., and Kuipers, J. a. M. Direct numerical simulation of flow and heat transfer in dense fluid-particle systems. *Chemical Engineering Science*, 81:329–344, 2012.

[5] Deen, N. G., Peters, E. a. J. F., Padding, J. T., and Kuipers, J. a. M. Review of direct numerical simulation of fluid-particle mass, momentum and heat transfer in dense gas-solid flows. *Chemical Engineering Science*, 116:710–724, 2014.

[6] Feng, Z.-G. and Michaelides, E. E. Heat transfer in particulate flows with Direct Numerical Simulation (DNS). *International Journal of Heat and Mass Transfer*, 52(3-4):777–786, 2009.

[7] Gunn, D. Transfer of heat or mass to particles in fixed and fluidised beds. *International Journal of Heat and Mass Transfer*, 21(4):467–476, 1978.

[8] Holloway, W., Yin, X., and Sundaresan, S. Fluid-Particle Drag in Inertial Polydisperse gas-solid Suspensions. *AIChE Journal*, 57(11):3199–3209, 2011.

[9] Kloss, C., Goniva, C., Hager, A., Amberger, S., and Pirker, S. Models, algorithms and validation for opensource DEM and CFD-DEM. *Progress in Computational Fluid Dynamics*, 12:140–152, 2012.

[10] Kriebitzsch, S. H. L., Hoef, M. A. V. D., and Kuipers, J. A. M. Drag Force in Discrete Particle Models-Continuum Scale or Single Particle Scale ? *AIChE Journal*, (59):315–324, 2012.

[11] Milioli, C. C., Milioli, F. E., Holloway, W., Agrawal, K., and Sundaresan, S. Filtered Two-Fluid Models of Fluidized Gas-Particle Flows: New Constitutive Relations. *AIChE Journal*, (59):3265–3275, 2013.

[12] Municchi, F., Radl, S., and Goniva, C. Highly efficient spatial data filtering in parallel using the opensource library CPPPO. *Computer Physics Communications (currently under review)*, 2016.

[13] Ranz, W. and Marshal, W. Evaporation from drops. *Chem. Eng. Prog.*, (48):141–146, 1952.

[14] Sankaran Sundaresan, Stefan Radl, Christian C. Milioli, F. E. M. Coarse-Grained Models for Momentum, Energy and Species Transport in Gas-Particle Flows. *The 14th International Conference on Fluidization-From Fundamentals to Products*, 2013.

[15] Schneiderbauer, S. and Pirker, S. A Coarse-Grained Two-Fluid Model for Gas-Solid Fluidized Beds. *The Journal of Computational Multiphase Flows*, 6(1):29–48, 2014.

[16] Tavassoli, H., Kriebitzsch, S., van der Hoef, M., Peters, E., and Kuipers, J. Direct numerical simulation of particulate flow with heat transfer. *International Journal of Multiphase Flow*, 57:29–37, 2013.

[17] Tavassoli, H., Peters, E., and Kuipers, J. Direct numerical simulation of fluid-particle heat transfer in fixed random arrays of non-spherical particles. *Chemical Engineering Science*, 129:42–48, 2015.

[18] Tenneti, S. and Subramaniam, S. Particle-Resolved Direct Numerical Simulation for Gas-Solid Flow Model Development. *Annual Review of Fluid Mechanics*, 46:199–230, 2014.

[19] Whitaker, S. Forced Convection Heat Transfer Correlations for Flow In Pipes, Past Flat Plates, Single. *AIChE Journal*, 18(2):361–371, 1972.